Thermodynamics and High-Pressure Kinetics of a Fast Carbon Dioxide Fixation Reaction by a (2,6-Pyridinedicarboxamidato-hydroxo)nickel(II) Complex

Journal:	*Dalton Transactions*
Manuscript ID:	DT-COM-10-2013-053004.R2
Article Type:	Communication
Date Submitted by the Author:	09-Jan-2014
Complete List of Authors:	Troeppner, Oliver; University of Erlangen-Nuernberg, Department of Chemistry and Pharmacy Huang, Deguang; Harvard University, Department of Chemistry and Chemical Biology Holm, R H; Harvard University, Higgins Professor of Chemistry Ivanovic-Burmazovic, Ivana; University of Erlangen-Nuernberg,

Journal Name RSCPublishing

COMMUNICATION

Thermodynamics and High-Pressure Kinetics of a Fast Carbon Dioxide Fixation Reaction by a (2,6-Pyridinedicarboxamidato-hydroxo)nickel(II) Complex

Cite this: DOI: 10.1039/x0xx00000x

O. Troeppner,[a] D. Huang[b], R. H. Holm[b] and I. Ivanović-Burmazović [a]

Received 00th January 2012,
Accepted 00th January 2012

DOI: 10.1039/x0xx00000x

www.rsc.org/

The previously reported carbon dioxide fixation reaction by the planar terminal hydroxide complex $[Ni(pyN_2^{Me2})(OH)]^{1-}$ in DMF has been further characterized by determination of the equilibrium constant $K_{eq}^{298} = 2.4 \pm 0.2 \times 10^5$ M^{-1} and $K_{eq}^{223} = 1.3 \pm 0.1 \times 10^7$ M^{-1}, as well as the volume of activation for the CO_2 binding ($\Delta V_{on}^{\ddagger\ 223} = -21 \pm 3$ cm^3 mol^{-1}) and back decarboxylation ($\Delta V_{off}^{\ddagger\ 223} = -13 \pm 1$ cm^3 mol^{-1}) by high-pressure kinetics. The data are consistent with an earlier DFT computation, including the probable nature of the transition state, and support designation of the reaction as one of the most completely investigated carbon dioxide fixation reactions of any type.

Fixation and utilization of CO_2 is an increasingly prominent problem[1-4] not only because CO_2 is a contributor to the greenhouse effect, but also because of its importance as a potentially cheap, nontoxic and abundant source of renewable synthetic fuels.[5] There are many general approaches that can lead to a fixation and utilization of CO_2 to form energetically more valuable molecules like carbon monoxide, methanol or methane, ranging from photochemical[6-18]- to electrochemical[1, 5, 19-34]- to chemical reduction[35-43] pathways. They often involve a variety of transition metal centers as redox catalysts, ranging from rather expensive and rare metals like ruthenium[21] and platinum[44] to cheaper and more abundant ones like nickel[22, 45] and copper.[1] A number of metal complexes have been synthesized and investigated as possible mimics of naturally occurring carbon monoxide dehydrogenase (CODH), an enzyme catalyzing the reversible redox reaction $CO_2 + 2H^+ + 2e^- \rightleftharpoons CO + H_2O$ and either containing Mo-Cu-S or Ni-Fe-S active sites.[46-49]

Besides redox methods, carbon dioxide fixation can also be achieved through non-redox processes.[4] Of the latter, reactions of a terminal $M^{II/III}$-OH group with CO_2 to afford bridging carbonate and terminal or bridging bicarbonate products are well documented.[50-54] Nature utilizes such a reaction within the catalytic cycle of carbonic anhydrases, where the terminal hydroxo group at the four-coordinate Zn^{II} center plays a crucial role in the reversible hydration of CO_2.[55] Formation of a unidentate bicarbonate complex seems to be critical for an efficiency of that catalytic cycle.[56] Some of us have recently observed that members of a set of planar terminal hydroxo complexes derived from *N,N'*-2,6-disubstitutedphenyl-2,6-dicarboxamide pincer ligands react rapidly and completely with CO_2 in DMF to form η^1-bicarbonate products (Scheme 1).[3, 57] Reactions are second-order with rate constants (*ca.* 10^4-10^6 $M^{-1}s^{-1}$) that tend to decrease as the steric size of the phenyl R-substituents increase. The most notable feature is the second-order rate constant $k_{on} = 9.5 \times 10^5$ $M^{-1}s^{-1}$ for reaction 1 at 298 K (Table 1), extrapolated from measurements at lower temperatures.[3] $[Ni(pyN^{Me2})(OH)]^{1-}$ carries the smallest *ortho*-substituent in the set; the unsubstituted ligand forms octahedral $[Ni(pyN_2)_2]^{2-}$.[58]

Scheme 1. Reversible Carbon Dioxide Fixation Reaction Mediated by $[Ni(pyN_2^{R2})(OH)]^{1-}$.

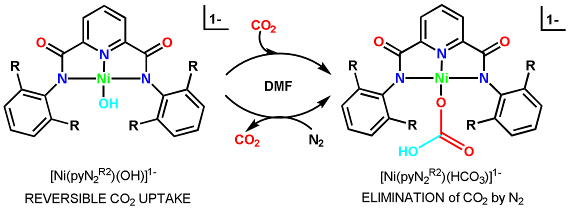

$$[Ni(py_{N2}^{Me2})(OH)]^{1-} + CO_2 \underset{k_{off}}{\overset{k_{on}}{\rightleftharpoons}} [Ni(py_{N2}^{Me2})(OCO_2H)]^{1-} \quad (1)$$

Table 1. Observed Equilibrium and Kinetic Parameters for the Reaction 1 of the R = CH_3 Complex in DMF.

K_{eq}^{298}	$2.4 \pm 0.2 \times 10^5$ M^{-1} [a]
K_{eq}^{223}	$1.3 \pm 0.1 \times 10^7$ M^{-1} [a]
k_{on}^{298}	9.5×10^5 $M^{-1}s^{-1}$ [b]
$\Delta H_{on}^{\ddagger}$	3.2 ± 0.5 kcal/mol [b]
$\Delta S_{on}^{\ddagger}$	-20 ± 3 cal/mol K [b]
$\Delta V_{on}^{\ddagger\ 223}$	-21 ± 3 cm^3/mol [a]
$\Delta V_{off}^{\ddagger\ 223}$	-13 ± 1 cm^3/mol [a]

[a]This work. [b]Ref. 3.

Comparison of k_{on}^{298} for reaction 1 with second-order rate constants for other systems including model reactions for the Zn(II) enzyme carbonic anhydrase reveals an increase of $\geq 10^3$ $M^{-1}s^{-1}$. Further, under the approximation $k_{on} \approx k_{cat}/K_M$ the rate constant overlaps the enzyme range of *ca.* 10^5-10^8 $M^{-1}s^{-1}$.[55] While precise comparisons cannot be made between synthetic or enzyme systems and reaction 1 owing to solvent differences (aqueous vs. DMF), it is nonetheless evident that this reaction is an unusually rapid CO_2 fixation process. Such rapid CO_2 fixation appears to be related to several notable features of $[Ni(pyN_2^{Me2})(X)]^-$: presence of the uncommon terminal Ni^{II}-OH group in the reactant and unidentate η^1-OCO_2H bicarbonate in the product complex, despite the four-coordinate ligand environment around the Ni^{II} center.[3]

Although the reversible character of this process has been qualitatively demonstrated,[57] quantification of this equilibrium and the back decarboxylation reaction has not yet been reported. Since efficiency of a CO_2 uptake is related to a CO_2 binding constant, the equilibrium constant K_{eq} of reaction 1 was thermodynamically and kinetically determined in this study at 298 K and 223 K, respectively, contributing to understanding of overall solution thermodynamics. Moreover, there is no literature data for binding constants of CO_2 to Ni-OH species. The only binding constant reported is for a Zn-hydroxo complex at 217 K.[53] Kinetics characterization of the reaction thus far has disclosed a low enthalpic barrier and a large negative entropy of activation consistent with a second-order reaction (Table 1). However, to fully comprehend the nature of this rather unique low activation pathway for CO_2 insertion, here we sought to determine the pressure effect on its kinetics, applying unique high-pressure cryo-temperature stopped-flow measurements at 223 K and 0.5-70 MPa. This is not only important in respect to the determination of a volume of activation ($\Delta V^{\neq}$) and thus visualization of a reaction transition state, but also considering an increase in solubility of CO_2 under low temperature and high pressure conditions, which can have an impact on efficiency of CO_2 sequestering on larger scales.

The compounds $(Et_4N)[Ni(pyN_2^{Me2})X]$ (X = OH^-, HCO_3^-) were prepared as described.[46, †] To elucidate the reversible nature of reaction 1 and to determine its equilibrium constant K_{eq}, a spectrophotometric titration was undertaken in which small aliquots of solutions of CO_2 in DMF were added to a 0.1 mM solution of $[Ni(pyN_2^{Me2})(OH)]^{1-}$ in DMF at 298 K in a 1 cm path-length septum-capped and gas-tight Uv/visible cuvette. Saturated solutions of CO_2 in DMF (0.2 M)[59, 60] were prepared by bubbling CO_2 gas at room temperature through argon-saturated dry DMF in a 10 mL gas-tight Hamilton syringe. Because the concentration of CO_2 required for the titration was not in a high excess over the complex concentration, spectrophotometric data were analyzed with eq 2 in which [ML] is the concentration of the product as a function of the concentration of CO_2 ($[L_0]$), $[M_0]$ is the total complex concentration and K_{eq} is the equilibrium constant. Change in the overall volume of a reaction mixture in the course of a titration is negligible because of the small amount of CO_2 titrant solution added. After the addition of CO_2 and prior to an absorbance measurement, the reaction mixture was allowed to equilibrate for 20 s.

$$[\boldsymbol{ML}] = \frac{\mathbf{1} + \boldsymbol{K_{eq}}([\boldsymbol{M_0}] + [\boldsymbol{L_0}]) - \sqrt{\left(\mathbf{1} + \boldsymbol{K_{eq}}([\boldsymbol{M_0}] + [\boldsymbol{L_0}])\right)^2 - \mathbf{4}\boldsymbol{K_{eq}}^2[\boldsymbol{M_0}][\boldsymbol{L_0}]}}{\mathbf{2}\boldsymbol{K_{eq}}} \qquad (2)$$

The UV/visible spectra obtained in the course of the titration are depicted in Figure 1 (left). Observed absorbance changes and tight isosbestic points at 279 and 395 nm are consistent with previous results[3] describing the expected single-step reaction; concentration of the product vs. $[CO_2]$ is shown in Figure 1 (right). Analysis of the global spectra data with eq 2 leads to $K_{eq}^{298} = 2.4 \pm 0.2 \times 10^5$ M^{-1}.

Using $K_{eq} = k_{on}/k_{off}$, we estimate the first order rate constant k_{off} for the back decarboxylation reaction to be 4 s^{-1} at 298 K. We have previously demonstrated the reversibility of the binding reaction by its reversal upon passing dinitrogen through a solution of $[Ni(pyN_2^{Me2})(OCO_2H)]^{1-}$.[3, 57]

The only other quantified equilibrium for CO_2 fixation is bicarbonate formation by CO_2 insertion in a Zn-OH bond ($K_{eq} = 6 \pm 2 \times 10^3$ M^{-1} in dichloromethane at 217 K, corresponding to $\Delta G = -3.8 \pm 0.2$ kcal/mol).[53] Under comparable low temperature conditions in DMF, reaction 1 is three to five orders of magnitude more efficient with estimated binding constants in the 4 x 10^7 to 8 x 10^8 M^{-1} range. The values were estimated from our K_{eq} value and reaction enthalpies previously computed with BP86 and B3LYP functionals, respectively.[3]

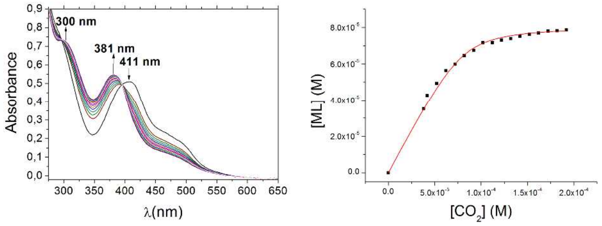

Figure 1. UV/visible spectral changes upon addition of small aliquots of CO_2 in DMF to a 0.l mM solution of $[Ni(pyN_2^{Me2})(OH)]^{1-}$ in DMF at room temperature (left). Plot of the concentration changes of the bicarbonate reaction product ([ML], based on the absorbance change at 381 nm) as dependent on $[CO_2]$; the red line is a fit to eq 2 (right).

In terms of the mechanism of reaction 1, one can envision either a transition state that is less or more compact than the product η^1-OCO_2H bicarbonate complex. The former will speak in favour of a four-coordinate transition state (hydroxo attack on CO_2 followed by a proton transfer),[61] whereas the latter supports a five-coordinate transition state (insertion of a carbon dioxide C-O bond into the Ni-OH bond).[3] This ambiguity is possible to overcome by determining the volume of activation, $\Delta V^{\neq}$, which will offer a clearer picture of the transition state in the solution. Given the information potentially forthcoming from effects of applied pressure on reaction rates,[62-64] the high-pressure kinetics of reaction 1 was investigated. To determine the activation volume $\Delta V^{\neq}$, pressure-dependent stopped-flow spectrophotometry at low temperature was employed.[‡] The decrease in absorbance of the Ni^{II} complex at 450 nm and constant temperature, during a course of CO_2 binding, was monitored within a pressure range of 0.5 - 70 MPa (Figure 2).

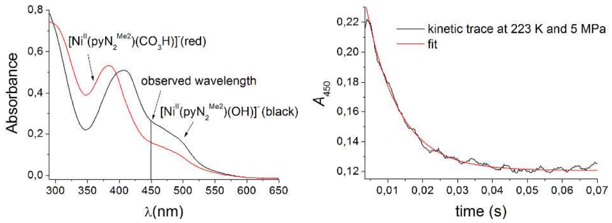

Figure 2. Spectral changes upon the reaction of 1 mM CO_2 and 0.1 mM $[Ni(pyN_2^{Me2})(OH)]^{1-}$ in DMF at room temperature (left). The kinetics trace (black) overlaid with the one-exponential fit to the data (red) for the same reaction system at 223 K and 0.5 MPa (right).

Reactions were performed under pseudo-first-order conditions, with CO_2 concentrations ranging between 0.5 and 1.5 mM and a Ni^{II} concentration of 0.1 mM. The temperature of the reaction cell and the solutions was maintained at 223 ± 0.1 K. Table S1 contains the resulting second order rate constants (k_{on}) derived from the slopes of plots of the observed rate constants as a function of CO_2 concentration at variable pressures (Figure 3 (left)). At least five kinetics runs were performed per data point up to 70 MPa at 223 K. Under these conditions, the volume of activation is independent of pressure and can be evaluated from the slope of the linear plot ($\ln(k_{on})$ vs. pressure)[62] in Figure 3 (right).[35]

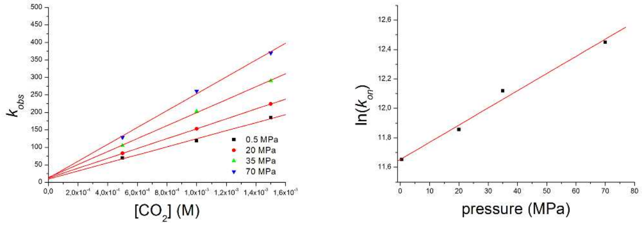

Figure 3. Plots of the observed rate constants (k_{obs}) as a function of CO_2 concentration at different pressures; 0.1 mM $[Ni(pyN_2^{Me2})(OH)]^{1-}$ in DMF at 223 K (left). Corresponding plot of $\ln(k_{on})$ vs. pressure (right).

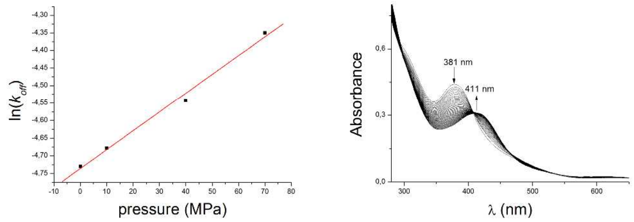

Figure 4. Plot of $\ln(k_{off})$ vs. pressure for the reaction of 0.08 mM $[Ni(pyN_2^{Me2})(OH)]^{1-}$ with CO_2 in DMF at 223 K (left). Corresponding time resolved UV/visible spectra on a course of the back decarboxylation reaction; 100 s observation time (right).

Analysis of the data leads to $\Delta V_{on}^{\ddagger} = -21 \pm 3$ cm^3 mol^{-1} for reaction 1. This value is entirely consistent with the negative value of $\Delta S^{\ddagger}$ for this reaction (Table 1) and supports an associative mechanism where bond breaking does not have a significant role in the rate-determining step. Unlike many classical substitution reactions, there is neither a leaving ligand nor a change in charge. Thus, the observed $\Delta V^{\neq}$ corresponds to the intrinsic volume change and directly reflects the transition state at the molecular level. Activation volumes for the same type of reaction are reported only for CO_2 uptake by $[M(NH_3)_5(OH)]^{2+}$ complexes in aqueous solution (M = Co^{III}, -10.1 ± 0.6; Rh^{III}, -4.7 ± 0.8; Ir^{III}, -4 ± 1 cm^3 M^{-1}).[61] These values are significantly less negative than that of reaction 1, suggesting a more compact transition state in that reaction. By way of comparison, the partial molar volume of CO_2 in DMF is ca. 43 cm^3 M^{-1}.[65] By a dilution experiment (stopped-flow mixing of $[Ni(pyN_2^{Me2})(OCO_2H)]^{1-}$ with degassed DMF at 223 K) at variable pressures we have directly determined the activation volume for the back decarboxylation reaction $\Delta V_{off}^{\ddagger} = -13 \pm 1$ cm^3 mol^{-1} (Figure 4, Table S1). This enabled us to construct a volume profile (Figure 5), which clearly indicates that the $\{[Ni(pyN_2^{Me2})(OH)]^{1-}\cdots CO_2\}^{\ddagger}$ transition state is more compact than the product bicarbonate complex. In addition, based on the kinetic parameters at 223 K (Table S1) the corresponding binding constant could be obtained as $K_{eq}^{223} = k_{on}/k_{off} = 1.3 \pm 0.1 \times 10^7$ M^{-1}, which is in accordance to the estimations based on the thermodynamic parameters (*vide supra*).

Such a volume profile supports a five-coordinate transition state with bidentate bicarbonate coordination on the way to the four-coordinate product.

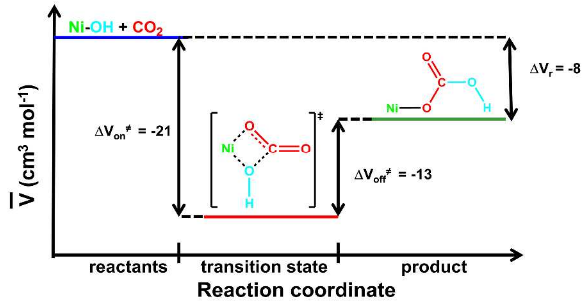

Figure 5. Volume profile for CO_2 fixation in reaction 1.

The four-coordinate structure of the starting complex and binding of the dinegative pincer ligand enhances the nucleophilicity of bound hydroxide. This favors initial nucleophilic attack of hydroxide and a cycloaddition pathway that should promote fast kinetics. The analogous reactions for the $[M(NH_3)_5(OH)]^{2+}$ systems (M = Co^{III}, Rh^{III} or Ir^{III})[61] have three orders of magnitude smaller rate constants than that in this study. This parallels a significantly lower nucleophility of OH$^-$ coordinated to the +3 metal centers within the positively charged $[M(NH_3)_5(OH)]^{2+}$ complexes in comparison to the nucleophility of OH$^-$ within negatively charged $[Ni(pyN_2^{Me2})(OH)]^{1-}$. The steric protection of the activated hydroxide and the increased electron density caused by the pincer ligand control the reaction thermodynamics and leads to a stable η^1-bound product. These collective features render CO_2 fixation by $[Ni(pyN_2^{Me2})(OH)]^{1-}$ kinetically and thermodynamically favorable. In addition to reaction 1,[3] the enthalpic reaction coordinate has also been computed by DFT methods for the slower reaction of CO_2 with $[Ni(pyN_2^{iPr2})(OH)]^{1-}$ ($k_{on} = 5.1 \times 10^4$ M^{-1}s^{-1}, $\Delta S^{\ddagger} = -27$ cal/mol K in DMF).[57] Results for both systems indicate a mechanism proceeding by nucleophilic attack at the carbon atom of CO_2 by hydroxide, formation of a cyclic transition state as depicted in Figure 5, rupture of one Ni-O bond, and reorientation of the resultant monodentate bicarbonate by a Ni-O-C pivot motion. The predicted final perpendicular orientation of bicarbonate relative to the NiN_3 plane is observed in crystalline salt of the reaction products.[46] The herewith visualized mechanism differs to that reported for $[M(NH_3)_5(OH)]^{2+}$ (M = Co^{III}, Rh^{III} or Ir^{III}),[61] where the rate-determining step in decarboxylation proceeds according to a dissociative mechanism that involves breakage of the oxygen-carbon bond on the carbonate ligand. In contrast, our back reaction has a clear associative character, involving a Ni-O bond formation and closure of a chelate bicarbonate ring. We should point out that the reactions between CO_2 and $[M(NH_3)_5(OH)]^{2+}$ operate in aqueous solutions, where a hydrogen-bonding network assists in proton transfer from bound hydroxide to one of the CO_2 oxygen atoms. On another hand, our reaction operates in DMF, within a hydrophobic environment of the sterically bulky ligand, and there is no possibility that the CO_2 oxygen atoms can be involved in some prominent hydrogen-bonding interactions. This makes the CO_2 oxygen atoms even more nucleophilic and prone to bound to the Ni^{II} center, resulting in a five-coordinate transition state. This may also explain the fact that our interpretation of the overall volume profile is consistent with, and may be said to support, the computed reaction pathway, although these computational models do not address hydrogen bonding.[3]

Conclusions

Here we have revealed the thermodynamics of the CO_2 binding to $[Ni(pyN_2^{Me2})(OH)]^-$, which was previously reported as the fastest CO_2 fixation reaction by metal-bound hydroxide.[3] Based on the determined equilibrium constant of $2.4 \pm 0.2 \times 10^5$ M^{-1} at 298 K and $1.3 \pm 0.1 \times 10^7$ M^{-1} at 223 K, it seems that thermodynamics of this process is also highly efficient, though there is limited literature information for comparisons.[53]

Our high-pressure kinetic studies revealed a large negative activation volume for both the CO_2 uptake and the back decarboxylation reaction. These results support a very compact transition state, which can be visualized as a five-coordinate species with bicarbonate bound in a bidentate fashion. The observed character of the transition state, in accordance with computational result,[3] explains a very low activation enthalpy and a negative activation entropy consistent with rapid CO_2 fixation. Reaction 1 is currently the most thoroughly characterized carbon dioxide fixation reaction by a metal hydroxide complex, and among the more completely examined carbon dioxide fixation reactions of any type.

Notes and references

[a] Department of Chemistry and Pharmacy, University of Erlangen-Nürnberg, Egerlandstr. 1 91058, Erlangen, Germany.
[b] Department of Chemistry and Chemical Biology, Harvard University, Cambridge, Massachusetts 02138, United States.
Corresponding Author. E-mail: ivana.ivanovic-burmazovic@fau.de, holm@chemistry.harvard.edu

Acknowledgements. I.I.-B., and O.T. gratefully acknowledge support through the "Solar Technologies Go Hybrid" initiative of the State of Bavaria. Research at Harvard University was supported by NIH Grant GM-28856.

† All manipulations and measurements were performed under a pure argon atmosphere. All reagents and solvents were purchased from commerical sources (Sigma-Aldrich, Acros Organics) and were of *p. a.* grade and used without purification. DMF was purchased as extra dry solvent and was stored in a sure-seal bottle under argon and molecular sieves. All solutions were prepared in dry DMF in an MBraun inert atmosphere glove box.

‡ Measurements were made using a Hi-Tech Scientific HPSF 56 stopped-flow instrument externally coupled to a Huber CC905 thermostat. UV/visible spectra were recorded using an Energetiq LDLS ENQ EQ-99 FC laser-driven light source coupled to an Applied Photo Physics photomultiplier. Solutions in DMF were prepared immediately before measurement. Lower concentrations of CO_2 were obtained by dilution of a saturated solution in graduated gas-tight syringes. Neither the solution of $[Ni(pyN_2^{Me2})OH)]^{1-}$ nor the CO_2 solution were exposed to the atmosphere.

Electronic Supplementary Information (ESI) available: [Rate constants for the CO_2 uptake (k_{on}) and decarboxylation (k_{off}) at elevated pressures]. See DOI:

1. Angamuthu, R.; Byers, P.; Lutz, M.; Spek, A. L.; Bouwman, E., *Science* **2010,** *327*, 313-5.
2. Sakakura, T.; Choi, J. C.; Yasuda, H., *Chemical Reviews* **2007,** *107*, 2365-87.
3. Huang, D.; Makhlynets, O. V.; Tan, L. L.; Lee, S. C.; Rybak-Akimova, E. V.; Holm, R. H., *Proceedings of the National Academy of Sciences of the United States of America* **2011,** *108*, 1222-7.
4. Appel, A. M.; Bercaw, J. E.; Bocarsly, A. B.; Dobbek, H.; Dubois, D. L.; Dupuis, M.; Ferry, J. G.; Fujita, E.; Hille, R.; Kenis, P. J.; Kerfeld, C. A.; Morris, R. H.; Peden, C. H.; Portis, A. R.; Ragsdale, S. W.; Rauchfuss, T. B.; Reek, J. N.; Seefeldt, L. C.; Thauer, R. K.; Waldrop, G. L., *Chemical Reviews* **2013,** *113*, 6621-6658.
5. Jitaru, M., *J. Univ. Chem. Technol. Metallurgy* **2007,** *42*, 333-334.
6. Takeda, H.; Koike, K.; Inoue, H.; Ishitani, O., *Journal of the American Chemical Society* **2008,** *130*, 2023-31.
7. Inoue, T.; Fujishima, A.; Konishi, S.; Honda, K., *Nature* **1979,** *277*, 637-638.
8. Thampi, K. R.; Kiwi, J.; Grätzel, M., *Nature* **1987,** *327*, 506-508.
9. Hawecker, J.; Lehn, J.-M.; Ziessel, R., *Journal of the Chemical Society, Chemical Communications* **1983**, 536.
10. Ikeue, K.; Yamashita, H.; Anpo, M.; Takewaki, T., *J. Phys. Chem. B* **2001,** *105*, 8350-8355.
11. Fujiwara, H.; Hosokawa, H.; Murakoshi, K.; Wada, Y.; Yanagida, S.; Okada, T.; Kobayashi, H., *J. Phys. Chem. B* **1997,** *101*, 8270-8278.
12. Grodkowski, J.; Dhanasekaran, T.; Neta, P.; Hambright, P.; Brunschwig, B. S.; Shinozaki, K.; Fujita, E., *J. Phys. Chem. A* **2000,** *104*, 11332-11339.
13. Ogata, T.; Yanagida, S.; Brunschwig, B. S.; Fujita, E., *Journal of the American Chemical Society* **1995,** *117*, 6708-6716.
14. Matsuoka, S.; Yamamoto, K.; Ogata, T.; Kusaba, M.; Nakashima, N.; Fujita, E.; Yanagida, S., *Journal of the American Chemical Society* **1993,** *115*, 601-609.
15. Hawecker, J.; Lehn, J.-M.; Ziessel, R., *Helvetica Chimica Acta* **1986,** *69*, 1990-2012.
16. Hori, H.; Johnson, F. P. A.; Koike, K.; Ishitani, O.; Ibusuki, T., *Journal of Photochemistry and Photobiology A: Chemistry* **1996,** *96*, 171-174.
17. Koike, K.; Hori, H.; Ishizuka, M.; Westwell, J. R.; Takeuchi, K.; Ibusuki, T.; Enjouji, K.; Konno, H.; Sakamoto, K.; Ishitani, O., *Organometallics* **1997,** *16*, 5724-5729.
18. Kurz, P.; Probst, B.; Spingler, B.; Alberto, R., *European Journal of Inorganic Chemistry* **2006,** *2006*, 2966-2974.
19. Jitaru, M.; Lowy, D. A.; Toma, M.; Toma, B. C.; Oniciu, L., *Journal of Applied Electrochemistry* **1997,** *27*, 875-889.
20. Aydin, R.; Köleli, F., *Journal of Electroanalytical Chemistry* **2002,** *535*, 107-112.
21. Begum, A.; Pickup, P. G., *Electrochemistry Communications* **2007,** *9*, 2525-2528.
22. Smith, C. I.; Crayston, J. A.; Hay, R. W., *Journal of the Chemical Society, Dalton Transactions* **1993**, 3267.
23. Dealwis, C., *Electrochimica Acta* **2000,** *45*, 2061-2074.
24. Gattrell, M.; Gupta, N.; Co, A., *Journal of Electroanalytical Chemistry* **2006,** *594*, 1-19.
25. Ikeda, S.; Takagi, T.; Ito, K., *Bulletin of the Chemical Society of Japan* **1987,** *60*, 2517-2522.
26. Isaacs, M.; Canales, J. C.; Riquelme, A.; Lucero, M.; Aguirre, M. J.; Costamagna, J., *Journal of Coordination Chemistry* **2003,** *56*, 1193-1201.
27. Kaneco, S.; Hiei, N.-h.; Xing, Y.; Katsumata, H.; Ohnishi, H.; Suzuki, T.; Ohta, K., *Electrochimica Acta* **2002,** *48*, 51-55.
28. Kaneco, S.; Iiba, K.; Hiei, N.-h.; Ohta, K.; Mizuno, T.; Suzuki, T., *Electrochimica Acta* **1999,** *44*, 4701-4706.
29. Kaneco, S.; Iwao, R.; Iiba, K.; Ohta, K.; Mizuno, T., *Energy* **1998,** *23*, 1107-1112.
30. Lee, J.; Kwon, Y.; Machunda, R. L.; Lee, H. J., *Chem Asian J* **2009,** *4*, 1516-23.
31. Lee, J.; Tak, Y., *Electrochimica Acta* **2001,** *46*, 3015-3022.
32. Schrebler, R.; Cury, P.; Herrera, F.; Gómez, H.; Córdova, R., *Journal of Electroanalytical Chemistry* **2001,** *516*, 23-30.
33. Schrebler, R.; Cury, P.; Suárez, C.; Muñoz, E.; Gómez, H.; Córdova, R., *Journal of Electroanalytical Chemistry* **2002,** *533*, 167-175.
34. Welford, P. J.; Brookes, B. A.; Wadhawan, J. D.; McPeak, H. B.; Hahn, C. E. W.; Compton, R. G., *J. Phys. Chem. B* **2001,** *105*, 5253-5261.
35. Kern, S.; van Eldik, R., *Inorg Chem* **2012,** *51*, 7340-5.
36. Creutz, C.; Chou, M. H., *Journal of the American Chemical Society* **2007,** *129*, 10108-9.
37. Dietrich, J.; Schindler, S., *Zeitschrift fur Anorganische und Allgemeine Chemie* **2008,** *634*, 2487-2494.
38. Inoue, Y.; Izumida, H.; Sasaki, Y.; Hashimoto, H., *Chemistry Letters* **1976**, 863-864.
39. Leitner, W., *Angewandte Chemie* **1995,** *107*, 2391-2405.
40. Jessop, P. G.; Hsiao, Y.; Ikariya, T.; Noyori, R., *Journal of the American Chemical Society* **1996,** *118*, 344-355.
41. Jessop, P. G.; Ikariya, T.; Noyori, R., *Nature* **1994,** *368*, 231-233.
42. Himeda, Y., *European Journal of Inorganic Chemistry* **2007,** *2007*, 3927-3941.

43. Laurenczy, G.; Joó, F.; Nádasdi, L., *Inorganic Chemistry* **2000,** *39*, 5083-5088.
44. Smolinka, T.; Heinen, M.; Chen, Y.; Jusys, Z.; Lehnert, W.; Behm, R., *Electrochimica Acta* **2005,** *50*, 5189-5199.
45. Simón-Manso, E.; Kubiak, C. P., *Organometallics* **2005,** *24*, 96-102.
46. Huang, D.; Holm, R. H., *Journal of the American Chemical Society* **2010,** *132*, 4693-701.
47. Ragsdale, S. W., *Critical Reviews in Biochemistry and Molecular Biology* **2004,** *39*, 165-95.
48. Ragsdale, S. W.; Kumar, M., *Chemical Reviews* **1996,** *96*, 2515-2540.
49. Lindahl, P. A., *Biochemistry* **2002,** *41*, 2097-2105.
50. Palmer, D. A.; Van Eldik, R., *Chemical Reviews* **1983,** *83*, 651-731.
51. Looney, A.; Han, R.; McNeill, K.; Parkin, G., *Journal of the American Chemical Society* **1993,** *115*, 4690-4697.
52. Kitajima, N.; Hikichi, S.; Tanaka, M.; Morooka, Y., *Journal of the American Chemical Society* **1993,** *115*, 5496-5508.
53. Sattler, W.; Parkin, G., *Polyhedron* **2012,** *32*, 41-48.
54. Bergquist, C.; Fillebeen, T.; Morlok, M. M.; Parkin, G., *Journal of the American Chemical Society* **2003,** *125*, 6189-99.
55. Zhang, X.; van Eldik, R., *Inorganic Chemistry* **1995,** *34*, 5606-5614.
56. Zhang, X.; van Eldik, R.; Koike, T.; Kimura, E., *Inorganic Chemistry* **1993,** *32*, 5749-5755.
57. Huang, D.; Makhlynets, O. V.; Tan, L. L.; Lee, S. C.; Rybak-Akimova, E. V.; Holm, R. H., *Inorg Chem* **2011,** *50*, 10070-81.
58. Patra, A. K.; Mukherjee, R., *Inorganic Chemistry* **1999,** *38*, 1388-1393.
59. Gennaro, A.; Isse, A. A.; Vianello, E., *Journal of Electroanalytical Chemistry and Interfacial Electrochemistry* **1990,** *289*, 203-215.
60. Tezuka, M.; Iwasaki, M., *Chemistry Letters* **1993**, 427-430.
61. Spitzer, U.; Van Eldik, R.; Kelm, H., *Inorganic Chemistry* **1982,** *21*, 2821-2823.
62. Van Eldik, R.; Asano, T.; Le Noble, W. J., *Chemical Reviews* **1989,** *89*, 549-688.
63. Hubbard, C. D.; van Eldik, R., *Inorganica Chimica Acta* **2010,** *363*, 2357-2374.
64. Van Eldik, R.; Dücker-Benfer, C.; Thaler, F., **1999,** *49*, 1-58.
65. Jödecke, M.; Pérez-Salado Kamps, Á.; Maurer, G., *Journal of Chemical & Engineering Data* **2012,** *57*, 1249-1266.